Dynamic Growth of Macroscopically Structured Supramolecular Hydrogels through Orchestrated Reaction-Diffusion

Wang, Hucheng; Fu, Xiaoming; Gu, Guanyao; Bai, Shengyu; Li, Runlai; Zhong, Weimin; Guo, Xuhong; Eelkema, Rienk; van Esch, Jan H.; Cao, Zhixing

DOI
10.1002/anie.202310162

Publication date
2023

Document Version
Final published version

Published in
Angewandte Chemie - International Edition

Citation (APA)
Wang, H., Fu, X., Gu, G., Bai, S., Li, R., Zhong, W., Guo, X., Eelkema, R., van Esch, J. H., Cao, Z., & Wang, Y. (2023). Dynamic Growth of Macroscopically Structured Supramolecular Hydrogels through Orchestrated Reaction-Diffusion. *Angewandte Chemie - International Edition*, *62*(43), Article e202310162. https://doi.org/10.1002/anie.202310162

How to cite: Angew. Chem. Int. Ed. 2023, e202310162
doi.org/10.1002/anie.202310162

Hydrogels

Dynamic Growth of Macroscopically Structured Supramolecular Hydrogels through Orchestrated Reaction-Diffusion

Hucheng Wang[+], Xiaoming Fu[+], Guanyao Gu, Shengyu Bai, Runlai Li, Weimin Zhong, Xuhong Guo, Rienk Eelkema, Jan H. van Esch, Zhixing Cao, and Yiming Wang**

Abstract: Living organisms are capable of dynamically changing their structures for adaptive functions through sophisticated reaction-diffusion processes. Here we show how active supramolecular hydrogels with programmable lifetimes and macroscopic structures can be created by relying on a simple reaction-diffusion strategy. Two hydrogel precursors (poly(acrylic acid) PAA/$CaCl_2$ and Na_2CO_3) diffuse from different locations and generate amorphous calcium carbonate (ACC) nanoparticles at the diffusional fronts, leading to the formation of hydrogel structures driven by electrostatic interactions between PAA and ACC nanoparticles. Interestingly, the formed hydrogels are capable of autonomously disintegrating over time because of a delayed influx of electrostatic-interaction inhibitors (NaCl). The hydrogel growth process is well explained by a reaction-diffusion model which offers a theoretical means to program the dynamic growth of structured hydrogels. Furthermore, we demonstrate a conceptual access to dynamic information storage in soft materials using the developed reaction-diffusion strategy. This work may serve as a starting point for the development of life-like materials with adaptive structures and functionalities.

[*] H. Wang,[+] G. Gu, S. Bai, Prof. X. Guo, Prof. Y. Wang
State Key Laboratory of Chemical Engineering, East China University of Science and Technology
Meilong Road 130, Shanghai 200237 (P. R. China)
E-mail: yimingwang@ecust.edu.cn

Dr. X. Fu,[+] Prof. W. Zhong, Prof. Z. Cao
Key Laboratory of Smart Manufacturing in Energy Chemical Process, East China University of Science and Technology
Meilong Road 130, Shanghai 200237 (P. R. China)
E-mail: zcao@ecust.edu.cn

Prof. Y. Wang
Shanghai Key Laboratory for Intelligent Sensing and Detection Technology, East China University of Science and Technology
Meilong Road 130, Shanghai 200237 (P. R. China)

Dr. R. Eelkema, Prof. J. H. van Esch
Department of Chemical Engineering, Delft University of Technology
van der Maasweg 9, 2629 HZ, Delft (The Netherlands)

Dr. R. Li
Department of Chemistry, National University of Singapore
Singapore 119077 (Singapore)

[+] These authors contributed equally to this work.

Introduction

Life is a sophisticated non-equilibrium supramolecular system, where the self-assembly is usually orchestrated by complex reaction-diffusion processes involving the transport of energy and matter,[1] resulting in a variety of elaborate supramolecular structures capable of growing and functioning in time and space.[2] Inspired by the dynamic biological system, many efforts have been made for the fabrication of synthetic supramolecular materials bearing time-dependent evolution of structures and properties. A milestone advance is the development of chemically fueled dissipative supramolecular self-assembly systems.[3] In these artificial systems, the input of chemical fuels converts the non-assembling building blocks into activated forms that can self-assemble into ordered structures, such as fibers,[4] vesicles,[5] and microdroplets.[6] However, once the fuels are depleted, these already formed structures cannot further survive and spontaneously disassemble over time, resembling the dynamic self-assembly phenomena observed in nature. Despite these advances, most of the resultant supramolecular structures remain to be limited at the level of assemblies due to the lack of diffusion control which is key to the structural growth of self-assembled materials.

To grow supramolecular materials with defined structures, people have coupled the self-assembly process with reaction-diffusion control.[7] van Esch et al. distributed gelator precursors in a polymer hydrogel substrate, by which formation and self-assembly of gelators were activated at the regions that the precursors met and reacted, resulting in free-standing supramolecular hydrogels with controlled shapes and sizes.[8] Smith's group studied diffusion of gelators across the interface of two solid gels, yielding interpenetrated self-assembled structures at the gel-gel interface;[9] they further proposed a double diffusion strategy that involves the diffusion of protons and pH-sensitive gelators in a polymer hydrogel substrate, giving rise to supramolecular hydrogels with well-defined shapes and sizes at the proton fronts.[10] In another example reported by Shi et al., the self-assembly of polyaminosaccharide chitosan was locally activated at the electrode areas by electrical signals, leading to hydrogels with multilayer structures.[11] Riedel-Kruse's group reported on their access to the programming of multicellular interface patterns using a synthetic cell-cell adhesion logic with swarming bacteria.[12] Nevertheless, in all these cases, the ultimately resultant supramolecular structures at the macroscopic level reside in a static state that is devoid of dynamic evolution behavior. Recently, Szalai and

colleagues pioneered a multi-channel hydrogel reactor by which various non-equilibrium outcomes, including oscillatory patterns, varying metal–organic frameworks (MOFs), were gained through control over the continuous supply of reactants in the channels.[13] Very recently, Walther's group reported on transient pH flip using enzymatic reaction networks in layered hydrogels, achieving transient self-assembly of pH-sensitive gelators.[14] However, achieving growth of both dynamic and macroscopic supramolecular structures in a closed system remains a formidable task.

Here we show our access to the dynamic growth of supramolecular hydrogels with control over their lifetime and structures by integrating the self-assembly and disassembly of the hydrogels in a reaction-diffusion process. The disassembly process is orchestrated to lag behind the self-assembly process through a delayed inhibiting effect. As such, hydrogel structures are formed at the locations of reaction and thereon disintegrate over time due to the gradually enhanced concentration gradient of inhibitors. A reaction-diffusion model that can well explain the dynamic growth process of the hydrogels is developed, offering a theoretical handle to rationally define the growth of the hydrogel structures. Furthermore, we harness the reaction-diffusion-governed structural growth of macroscopic hydrogels for transient patterning, demonstrating an interesting paradigm of dynamic information storage in soft materials.

The self-assembling system we used in this study is a mineralized supramolecular hydrogel consisting of poly(acrylic acid) (PAA) and amorphous calcium carbonate (ACC) nanoparticles (Figure S1). By simply mixing an aqueous solution of Na_2CO_3 with PAA/$CaCl_2$, PAA/ACC hydrogel can be formed due to the strong electrostatic interaction between PAA chains and the in situ formed ACC nanoparticles, which has been systematically investigated by Sun et al.[15] Interestingly, the hydrogel disintegrates over time with the addition of sufficient counterions (Na^+) (Figure 1a and S2), which is explained by the electrostatic screening effect. As shown in Figure 1b, we propose that the aqueous solutions of Na_2CO_3 and PAA/$CaCl_2$ deposited at separated locations in a diffusion medium would diffuse to meet and react at a prescribed region, leading to the self-assembly of PAA/ACC hydrogels there; and the presence of an appropriate amount of Na^+ may result in the growth followed by disintegration of the hydrogels.

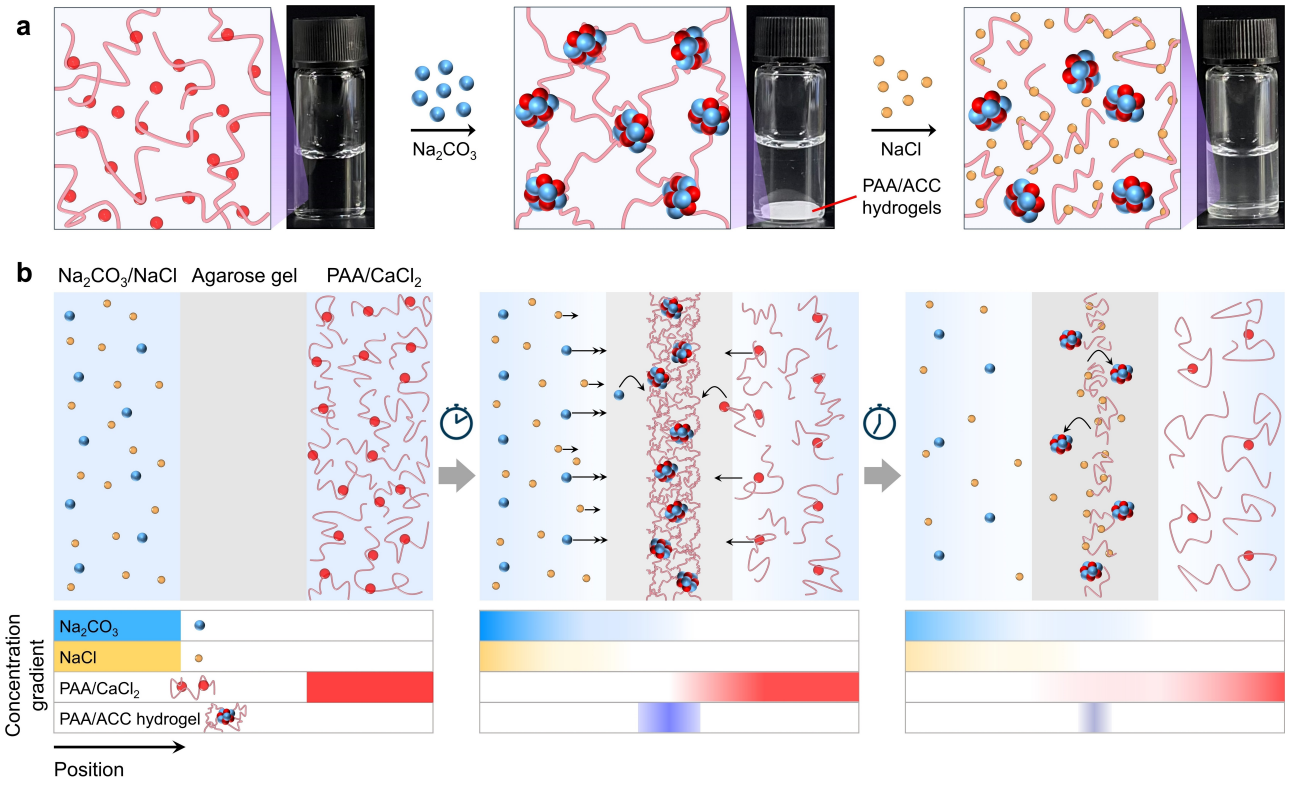

Figure 1. Illustration of the dynamic growth of PAA/ACC hydrogels through orchestrated reaction-diffusion. a) Self-assembly and disassembly of PAA/ACC hydrogels resulting from the in situ formation of ACC nanoparticles and electrostatic screening effect of Na^+, respectively; b) Scheme showing the dynamic self-assembly of the PAA/ACC hydrogels and the concentration evolution of each species in space and time: Na_2CO_3 and PAA/$CaCl_2$ first diffuse from separated locations and self-assemble into PAA/ACC hydrogels upon reaction at the diffusional front; meanwhile, the concentration gradient of NaCl gradually increases to the level that makes the disassembly dominant, thereby resulting in the degradation of the already formed hydrogels. Sample in (a): 3 mL Na_2CO_3 (0.1 M), 5 mL PAA/$CaCl_2$ (0.2 M/0.1 M, pH 3.5), and 1 mL NaCl (0.8 M).

Results and Discussion

We first coupled the PAA/ACC hydrogel system to a simple one-dimensional (1D) reaction-diffusion case where aqueous solutions of PAA/$CaCl_2$ and Na_2CO_3 are separated by a diffusion medium made by 1.0 wt% agarose gel (Figure 2a). Here PAA/$CaCl_2$ was treated as a single component because of the high affinity of cationic Ca^{2+} to anionic PAA, which is pre-mixed for complete formation of the electrostatic complex. Samples with different pH and compositions were prepared for the reaction-diffusion tests to seek the optimal experiment conditions (Figure S3). Interestingly, 1D white lines close to the PAA/$CaCl_2$ reservoir were formed ultimately in each sample, which is demonstrated to be PAA/ACC hydrogels (Figure S4). The formation of hydrogel close to the PAA/$CaCl_2$ reservoir is attributed to the slower diffusion of PAA/$CaCl_2$. In some cases, coarse white lines near the middle of the agarose gel were observed, which are determined to be $CaCO_3$ crystals formed by the trace $CaCl_2$ that are not interacted with PAA chains (Figure S3 and S5). Taken together, the PAA/$CaCl_2$ (0.114 M/0.02 M) solution at pH 3.5 and Na_2CO_3 (0.02 M) were selected as the optimal conditions for the following study as pure $CaCO_3$ crystals are minimally formed. The concentrations of the reactants in this work refer to the concentrations of added solutions.

Next, we devoted to investigating the dynamic growth of the PAA/ACC hydrogel by introducing different amounts of NaCl into the Na_2CO_3 reservoir. As shown in Figure 2b–2d, a PAA/ACC hydrogel line was formed after ≈5 h for the sample without NaCl (Movie S1). Over time, the width of the hydrogel (Figure S6) further increased till reaching a plateau of ≈2.1 mm after ≈37 h (Figure 2c). When we increased [NaCl] from 0 to 0.2 M, the resultant PAA/ACC hydrogel gave rise to lower plateau width, which can be attributed to the enhanced inhibiting effect of Na^+ (Figure 2d). However, once [NaCl] reaches 0.3 M, the hydrogel first grows to a maximum width of ≈1.2 mm at ≈15 h and subsequently disintegrates over time (Movie S1), showing a tangible transient feature. This can be explained by the sufficient inhibiting effect at higher [NaCl] that disrupts the electrostatic interaction between PAA and ACC nanoparticles. Further increasing [NaCl] from 0.3 to 0.6 M, a series of dynamic hydrogels with much lower plateau width (decreasing from ≈1.2 to ≈0.9 mm, respectively) and shorter lifetime (decreasing from ≈40 to ≈17 h, respectively) were obtained (Figure 2d). Furthermore, our reaction-diffusion system also allows for control over the dynamic hydrogel growth by changing the width of the agarose gel substrate and the distribution of NaCl in the two separated reservoirs, which has been investigated and discussed in the Supporting Information (Figure S7 and S8).

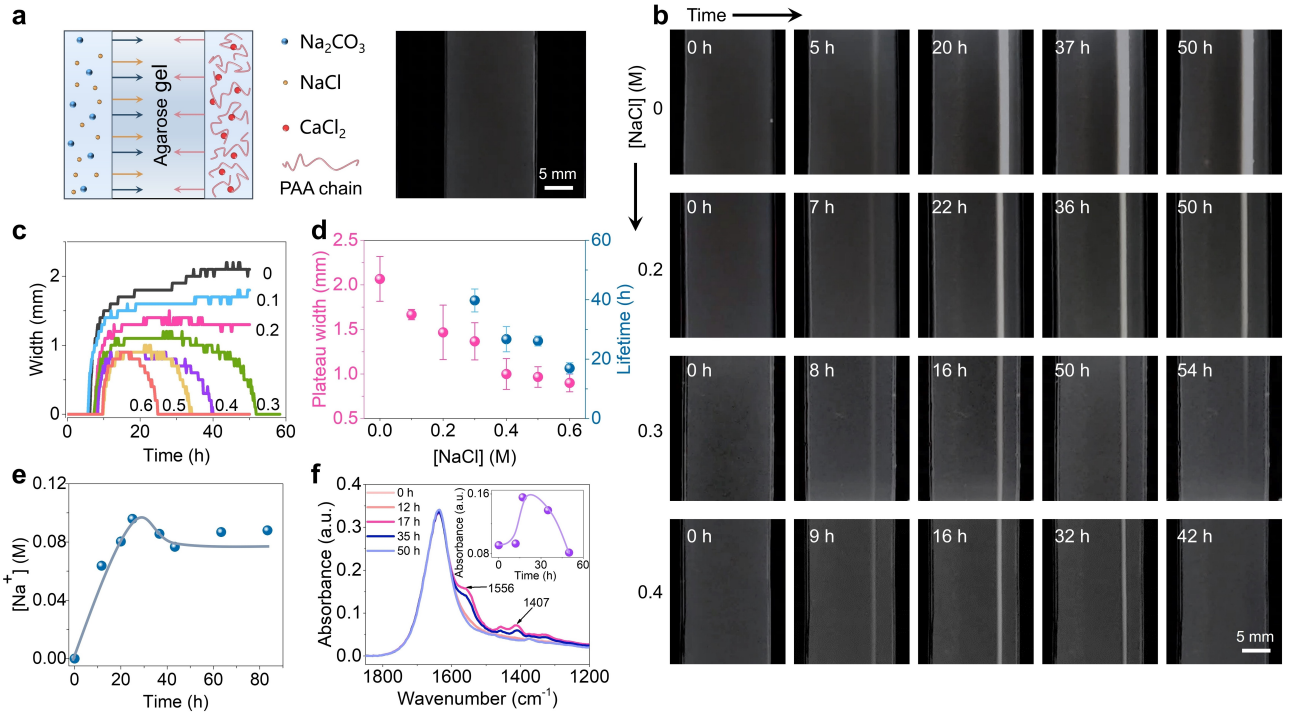

Figure 2. Dynamic growth of 1D supramolecular PAA/ACC hydrogels. a) The formation of a 1D PAA/ACC hydrogel through reaction-diffusion in a 1.0 wt% agarose gel medium; b) snapshots showing the growth process of PAA/ACC hydrogels and c) variation of the hydrogel width over time with different [NaCl]; d) plateau width and lifetime of the hydrogels as a function of [NaCl], the error bars are s.d. calculated from three parallel tests; e) evolution of $[Na^+]$ over time at the region of hydrogel formation, the line is added to guide the eyes; f) ATR-IR spectra showing the dynamic growth process of PAA/ACC hydrogels. Samples in (b)–(d): 2 mL PAA/$CaCl_2$ (0.114 M/0.02 M, pH 3.5) and 2 mL Na_2CO_3/NaCl (0.02 M/different [NaCl]), additional 0.4 M NaCl were used in (e) and (f).

It seems that when [NaCl] is higher than 0.3 M, the PAA/ACC hydrogel is allowed to grow in the beginning because the [Na^+] remains below the critical inhibiting level; however, upon the diffusion of NaCl and its accumulation at the hydrogel area for its affinity to the anionic PAA, the inhibiting effect gradually increases over the inhibiting level, thereby leading to the disintegration of the already formed hydrogel. To verify this hypothesis, we monitored the variation of [Na^+] at the region where the PAA/ACC hydrogel formed. The sample with the addition of 0.4 M NaCl was showcased for this test. The results showed that [Na^+] gradually increased from 0 to the maximum of ≈0.1 M within the first ≈25 h (Figure 2e), which is in line with the disintegration time of the hydrogel (Figure 2c). Interestingly, instead of reaching a plateau, [Na^+] thereon slightly decreased over time and leveled off at ≈0.08 M (Figure 2e). The slight decrease can be caused by the hydrogel disintegration by which the accumulated Na^+ was released. The evolution of [Na^+] at the hydrogel formed area is in excellent accordance with the dynamic growth process of the hydrogel. It should note that the dynamic hydrogel growth shows underwhelming recyclability by testing with either the same or increasing concentrations of the reactants after the first growth cycle (Figure S9), which can be explained by the accumulation of inhibitor NaCl in this closed system.

To further insight into the dynamic growth process of the hydrogels, attenuated total reflection infrared spectroscopy (ATR-IR) measurements were performed. As shown in Figure 2f, after ≈9 h, the absorption intensities at 1407 and 1556 cm^{-1} start to increase, which are caused by the formation of ACC nanoparticles and the interaction between PAA and the formed ACC nanoparticles, respectively, suggesting the formation of PAA/ACC hydrogel.[15a,16] After that, the intensity at 1556 cm^{-1}, for instance, continues to increase over time, indicating the further growth of the hydrogel. After reaching the maximum at ≈25 h, the intensity starts to decrease and recovers to the original level at ≈50 h, which is underpinned by the degradation of the hydrogel. Importantly, the temporal intensity variation is highly correlated to the evolutions of hydrogel width and the local [NaCl] as discussed above (Figure 2c and 2e), further demonstrating the proposed dynamic growing process of the PAA/ACC hydrogels.

Subsequently, we developed a reaction-diffusion model to describe the dynamic self-assembly process to allow us to rationally program the dynamic growth of the PAA/ACC hydrogels. In the model (see Supporting Information, Figure S10), Na_2CO_3/NaCl and PAA/$CaCl_2$ diffuse towards each other and activate the self-assembly at the diffusional fronts through the in situ formation of ACC nanoparticles; the hydrogel degradation process is triggered by the gradually elevated [Na^+]. The model parameters, including diffusion coefficients of all species, reaction and (dis)assembly rate constants are extracted by fitting against the experimental data of the evolution of hydrogel width over time in the presence of different [NaCl] (Table S1). For example, for the 1D hydrogel prepared with the addition of 0.4 M NaCl, the simulated hydrogel shows a compatible growing profile with the experiment (Figure 3a and Movie S2), and the width evolution of the hydrogel is quantitatively consistent with the experimental data (Figure 3b). Thanks to the model, the spatiotemporal variation of the concentrations of different species during the dynamic growth of the hydrogel are well predicted (Figure S11 and Movie S2). Besides, the established model was able to quantitatively predict both the width and lifetime of the hydrogels formed in the presence of different [NaCl] (Figure 3c and 3d), indicating the validity of the model. The model suggests that [NaCl] plays a dominant role in the dynamic growth of PAA/ACC hydrogels, both the plateau width and lifetime of the hydrogels decrease with an increase in [NaCl] (Figure 3d).

With the help of the established model, we are allowed to program the dynamic growth of the PAA/ACC hydrogels. We first focused on the structuralized growth of PAA/ACC hydrogels by simply changing the shape of the diffusion medium. In the simulation, a circular and a square diffusion media with prescribed sizes were defined, respectively (Figure S12). The model shows that circular and square PAA/ACC hydrogels are gradually formed and reach the maximum width at 25 and 16 h, respectively; thereon the formed hydrogels start to disintegrate and completely disappear at 75 and 45 h, respectively (Figure 3e, Movie S3 and S4). To validate the simulation results, we performed experiments using the same parameters. Notably, we found that the PAA/ACC hydrogels displayed comparable evolutions of structure, size, and lifetime with their simulation counterparts (Figure 3e, Movie S3 and S4).

We further employed the model to program the growth of PAA/ACC hydrogels by defining the locations of reaction-diffusion species in space without changing the shape of the diffusion medium (Figure S12). In a reaction-diffusion example with two defined square holes, we found that, as time elapsed, a bracket-like structure was transiently formed with a lifetime of ≈45 h (Figure 3f and Movie S5). By experimentally making the same reservoirs in agarose gel, PAA/ACC hydrogel with identical structure and lifetime was observed in the defined region. Moreover, by changing the combination of the number, location, and shape of the reservoirs, we are allowed to predictively grow dynamic PAA/ACC hydrogels with more complex structures (Figure 3f, Movie S6 and S7). Thus, the reaction-diffusion model not only furthers our understanding of the hydrogel growth process but also functions as a powerful tool to program the growth of structured PAA/ACC hydrogels.

Dynamic growth of soft structures through the exchange of substances is ubiquitous in the biological system, generating various advanced functions.[17] For instance, the brain stores the learned information through a dynamic memorizing-forgetting process,[18] which is considered to be a result of the exchange of substances, such as dopamine and proteins.[19] Inspired by such a non-equilibrium memorizing-forgetting process in the brain, we are curious about whether the reaction-diffusion-mediated dynamic hydrogel growth can serve as a manmade soft material platform for dynamic information storage. As shown in Figure 4a, we propose a soft contact printing strategy that the agarose gel with

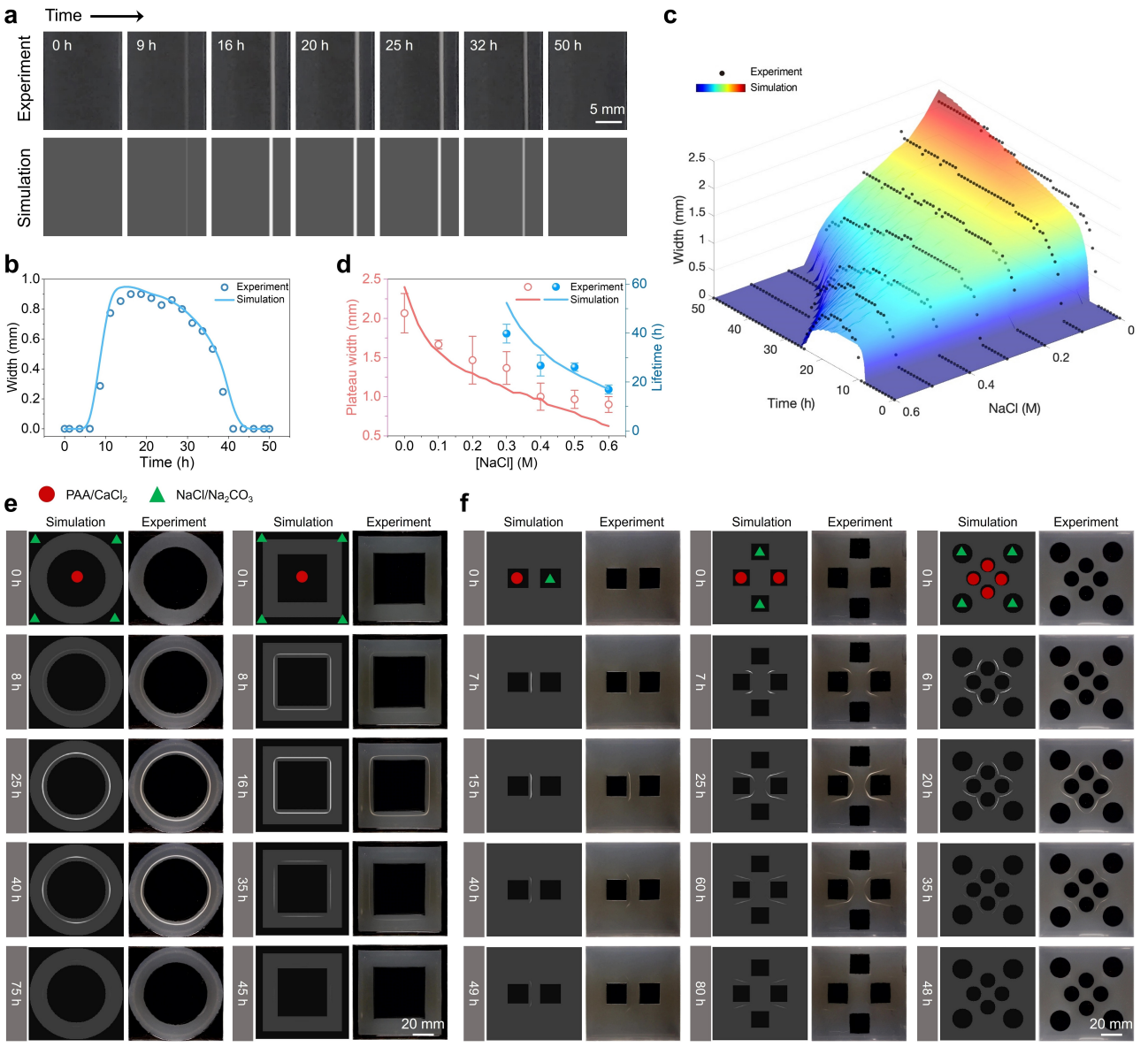

Figure 3. Programming the dynamic growth of structured PAA/ACC hydrogels using reaction-diffusion modeling. a–d) Comparison of simulation and experiment results for a) dynamic structure variation and b) width evolution of the 1D PAA/ACC hydrogel formed with the addition of 0.4 M NaCl; c, d) simulation and experimental results for the hydrogels formed with different [NaCl], error bars in (d) are s.d. calculated from three parallel tests; e, f) simulation guided programmable growth of dynamic PAA/ACC hydrogel structures. Samples in (e) and (f): red and green marks stand for PAA/$CaCl_2$ (0.114 M/0.02 M, pH 3.5) and Na_2CO_3/NaCl (0.02 M/0.5 M), respectively.

already formed PAA/ACC hydrogel inside serves as a soft substrate for information storage, and a soft stamp containing NaCl solutions made by agarose gel is used for writing patterns (information) in the soft substrate. We speculate that, upon printing, the NaCl diffuses from the stamp into the substrate, thereby leading to the disintegration of PAA/ACC hydrogel in the substrate at the printed area; however, the NaCl at the printed area will be diluted over time because of its spontaneous diffusion to the bulk, thus allowing for the rebuilding of the disintegrated PAA/ACC hydrogels. As such, various dynamic patterns (information) can be easily created in the PAA/ACC hydrogel with a finite lifetime.

To achieve the proposed dynamic information storage, the key is to control the [NaCl] in the printed area at an appropriate level, because too high [NaCl] will disable the recovery of the disintegrated PAA/ACC hydrogels while too low [NaCl] cannot disintegrate the hydrogel. In this context, we tested the dynamic patterning with varying [NaCl] and printing time (Figure S13). According to the results, we determined the optimal conditions ([NaCl] = 0.4 M, printing time = 5 min) in considering the quality and autonomous erasing capability of the patterns (Figure S14 and Movie S8). Under the optimal conditions, a clear pattern is created in the PAA/ACC hydrogel substrate after the printing (Figure 4b); however, interestingly, the pattern

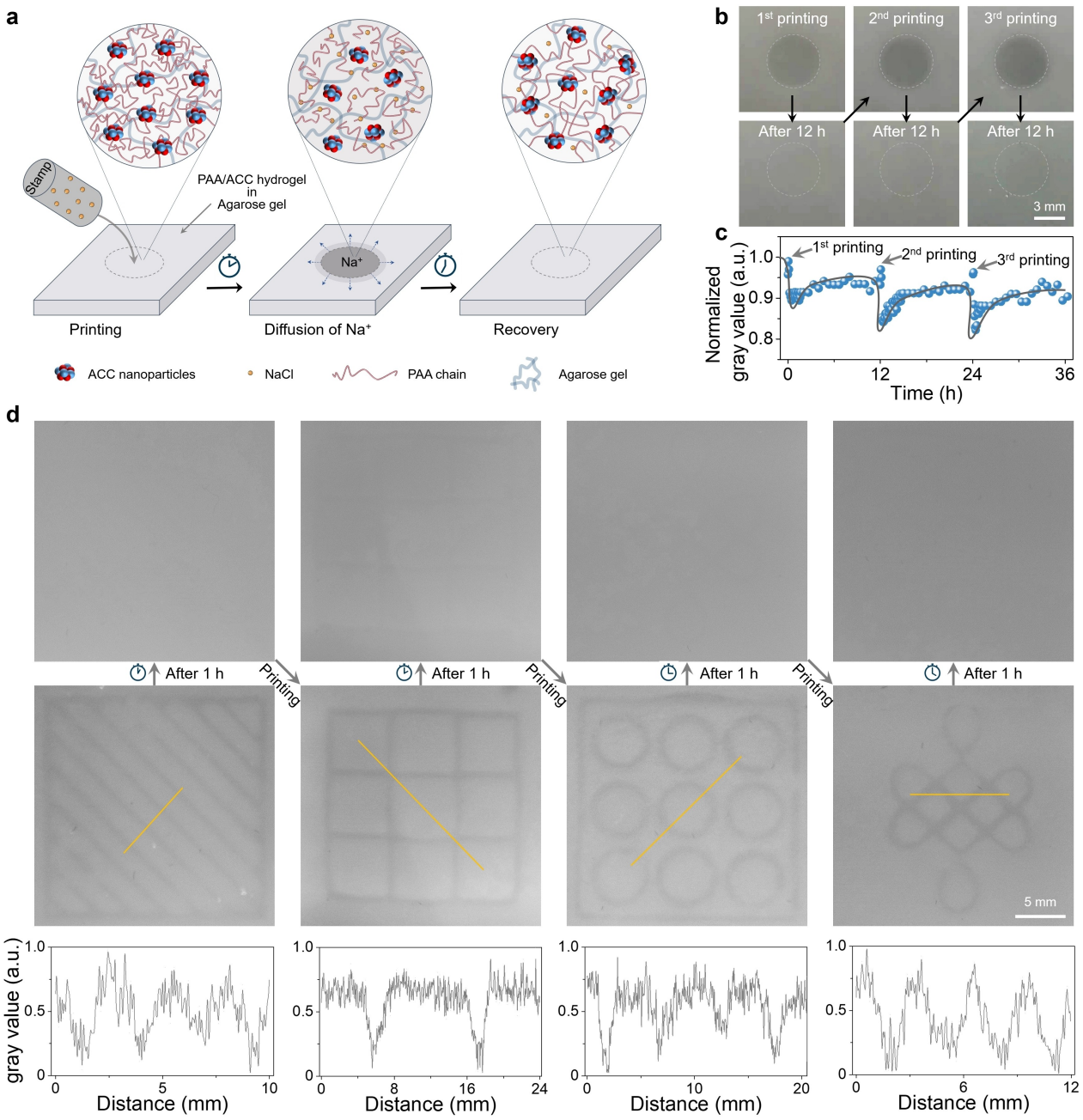

Figure 4. Dynamic memory in a PAA/ACC hydrogel substrate through dynamic patterning. a) Scheme showing the creation of dynamic patterns on PAA/ACC hydrogel substrates through soft contact printing using a stamp containing NaCl; b) snapshots of the stamping process and 3 cycles of printed patterns and c) normalized gray value evolution showing the dynamic and repeatable patterning process using a cylindrical stamp containing 0.4 M NaCl for 5 min printing; d) creation of differently shaped dynamic patterns (from left to right: stripes, squares, rings, and Chinese knot, respectively) in the same PAA/ACC hydrogel substrate using different stamps, and the top images are normalized gray intensity profiles corresponding to the yellow lines on the snapshots.

gradually vanishes against time with a recovery of normalized gray value from ≈0.88 to ≈0.98 (Figure 4c). Interestingly, the patterning process can be repeated at least three times with a slight loss in its self-erasing capability (Figure 4c), demonstrating the potential for dynamic and repeat information storage. We should note that the control samples devoid of diffusion of NaCl to the bulk are incapable of recovering after the disintegration of PAA/ACC hydrogel (Figure S15), in line with the proposed mechanism at play. After demonstrating the dynamic creation of patterns in PAA/ACC hydrogel substrate through the simple soft contact printing approach, various stamps with different shapes were used for the fabrication of more complex patterns. Thanks to the dynamic and excellent self-erasing capability of the patterning, as shown in Figure 4d, patterns including strips, squares, rings, and

Chinese knots can be easily created in the same PAA/ACC hydrogel substrate through multiple printing-self-erasing cycles (Movie S9), showing an interesting proof-of-concept application for life-like dynamic information storage. It is noteworthy that spatial control over the functions of materials using printing has been widely reported, for instance, Velev et al. realized the patterning and deformation of the hydrogels by ionoprinting and reversed the process by exposing the hydrogel to chelator solutions.[20] However, the recovery process is not spontaneous and requires to manually exposing the materials to certain inhibiting cues.

Conclusion

In summary, we have demonstrated a reaction-diffusion approach for the dynamic growth of supramolecular hydrogels with controlled structures and lifetimes, reminiscent of the dynamic organization of biological structures underpinned by complex reaction-diffusion processes. We couple a mineralized supramolecular hydrogel system composed of poly(acrylic acid) (PAA) and in situ formed amorphous carbonate calcium (ACC) nanoparticles to a reaction-diffusion system; upon orchestrating the self-assembly process triggered by the formation of ACC and the disassembly process resulting from counterions-caused electrostatic screening effect, we achieved the dynamic growth of the PAA/ACC hydrogels with controlled lifetimes and macroscopic structures. The dynamic growth of the hydrogels is well explained by a reaction-diffusion model which offers a tool to program the hydrogel growth and decay. Furthermore, we have demonstrated a proof-of-concept application of the dynamic growth of PAA/ACC hydrogels for dynamic information storage in soft substrates, partially resembling the dynamic memorizing-forgetting behavior of the brain. Such a reaction-diffusion strategy for the dynamic growth of structured supramolecular hydrogels may offer a route to develop new life-like soft materials with adaptive structures and functionalities, such as self-renewal and information encryption.

Acknowledgements

Y.W. acknowledge the financial support of the "Chenguang Program" supported by the Shanghai Education Development Foundation and Shanghai Municipal Education Commission (20CG36), Shanghai Special Program for Fundamental Research (22TQ1400100-9), National Key Research and Development Program of China (2022YFD70050101), and the Open Project of State Key Laboratory of Chemical Engineering (SKL-ChE-23C01); W.Z. acknowledges the support from NSFC (61925305); Z.C. acknowledges the support from NSFC (62073137), Shanghai Action Plan for Technological Innovation Grant (22ZR1415300, 22511104000) and Shanghai Center of Biomedicine Development; X.F. acknowledges the support from the fellowship of China Post-doctoral Science Foundation (2021M071202) and the support from Shanghai Sailing Program (22YF1410700).

Conflict of Interest

The authors declare no conflict of interest.

Data Availability Statement

The data that support the findings of this study are available from the corresponding author upon reasonable request.

Keywords: Hydrogels · Non-Equilibrium Systems · Reaction-Diffusion · Self-Assembly · Supramolecular Materials

[1] a) Y. Sasai, *Nature* **2013**, *493*, 318–326; b) A. N. Landge, B. M. Jordan, X. Diego, P. Muller, *Dev. Biol.* **2020**, *460*, 2–11.
[2] a) F. Crick, *Nature* **1970**, *225*, 420–422; b) P. R. Clarke, *Science* **2005**, *309*, 1334–1335; c) R. Villanueva, M. Coll-Llado, L. Bonnaud-Ponticelli, S. A. Carrasco, O. Escolar, F. A. Fernandez-Alvarez, I. G. Gleadall, J. Nabhitabhata, N. Ortiz, C. Rosas, P. Sanchez, J. R. Voight, J. Swoger, *Front. Mar. Sci.* **2021**, *8*, 645738.
[3] a) J. Boekhoven, A. M. Brizard, K. N. K. Kowlgi, G. J. M. Koper, R. Eelkema, J. H. Van Esch, *Angew. Chem. Int. Ed.* **2010**, *49*, 4825–4828; b) J. Boekhoven, W. E. Hendriksen, G. J. M. Koper, R. Eelkema, J. H. Van Esch, *Science* **2015**, *349*, 1075–1079; c) S. A. P. Van Rossum, M. Tena-Solsona, J. H. Van Esch, R. Eelkema, J. Boekhoven, *Chem. Soc. Rev.* **2017**, *46*, 5519–5535; d) S. De, R. Klajn, *Adv. Mater.* **2018**, *30*, 1706750; e) K. Das, L. Gabrielli, L. J. Prins, *Angew. Chem. Int. Ed.* **2021**, *60*, 20120–20143; f) Q. Wang, Z. Qi, M. Chen, D. H. Qu, *Aggregate* **2021**, *2*, e110.
[4] a) S. Debnath, S. Roy, R. V. Ulijn, *J. Am. Chem. Soc.* **2013**, *135*, 16789–16792; b) C. A. Angulo-Pachon, J. F. Miravet, *Chem. Commun.* **2016**, *52*, 5398–5401; c) X. Q. Xie, Y. Zhang, Y. Liang, M. Wang, Y. Cui, J. Li, C. S. Liu, *Angew. Chem. Int. Ed.* **2022**, *61*, e202114471.
[5] a) R. Tamate, T. Ueki, M. Shibayama, R. Yoshida, *Angew. Chem. Int. Ed.* **2014**, *53*, 11248–11252; b) S. Maiti, I. Fortunati, C. Ferrante, P. Scrimin, L. J. Prins, *Nat. Chem.* **2016**, *8*, 725–731; c) B. P. Bastakoti, J. Perez-Mercader, *Adv. Mater.* **2017**, *29*, 1704368.
[6] a) M. Tena-Solsona, C. Wanzke, B. Riess, A. R. Bausch, J. Boekhoven, *Nat. Commun.* **2018**, *9*, 2044; b) Y. D. Yin, L. Niu, X. C. Zhu, M. P. Zhao, Z. X. Zhang, S. Mann, D. H. Liang, *Nat. Commun.* **2016**, *7*, 10658.
[7] a) B. A. Grzybowski, W. T. S. Huck, *Nat. Nanotechnol.* **2016**, *11*, 585–591; b) L. Cera, C. A. Schalley, *Adv. Mater.* **2018**, *30*, 1707029; c) R. Chen, K. Das, M. A. Cardona, L. Gabrielli, L. J. Prins, *J. Am. Chem. Soc.* **2022**, *144*, 2010–2018; d) Y. Wei, S. Han, D. A. Walker, P. E. Fuller, B. A. Grzybowski, *Angew. Chem. Int. Ed.* **2012**, *51*, 7435–7439; e) J. H. Park, J. Paczesny, N. Kim, B. A. Grzybowski, *Angew. Chem. Int. Ed.* **2020**, *59*, 10301–10305.
[8] M. Lovrak, W. E. J. Hendriksen, C. Maity, S. Mytnyk, V. Van Steijn, R. Eelkema, J. H. Van Esch, *Nat. Commun.* **2017**, *8*, 15317.
[9] L. Schlichter, C. C. Piras, D. K. Smith, *Chem. Sci.* **2021**, *12*, 4162–4172.

[10] H. S. Cooke, L. Schlichter, C. C. Piras, D. K. Smith, *Chem. Sci.* **2021**, *12*, 12156–12164.
[11] K. Yan, F. Ding, W. E. Bentley, H. Deng, Y. Du, G. F. Payne, X. W. Shi, *Soft Matter* **2014**, *10*, 465–469.
[12] H. Kim, D. J. Skinner, D. S. Glass, A. E. Hamby, B. A. R. Stuart, J. Dunkel, I. H. Riedel-Kruse, *Nature* **2022**, *608*, 324–329.
[13] a) B. Dúzs, I. Szalai, *Commun. Chem.* **2020**, *3*, 168; b) B. Dúzs, G. Holló, G. Schuszter, D. Horváth, Á. Tóth, I. Szalai, I. Lagzi, *Sci. Rep.* **2022**, *12*, 222; c) B. Dúzs, I. Szalai, *Phys. Chem. Chem. Phys.* **2022**, *24*, 1814–1820.
[14] X. L. Fan, A. Walther, *Angew. Chem. Int. Ed.* **2021**, *60*, 3619–3624.
[15] a) S. T. Sun, L. B. Mao, Z. Y. Lei, S. H. Yu, H. Colfen, *Angew. Chem. Int. Ed.* **2016**, *55*, 11765–11769; b) Y. Oaki, S. Kajiyama, T. Nishimura, H. Imai, T. Kato, *Adv. Mater.* **2008**, *20*, 3633–3637; c) T. Saito, Y. Oaki, T. Nishimura, A. Isogai, T. Kato, *Mater. Horiz.* **2014**, *1*, 321–325.
[16] D. Gebauer, P. N. Gunawidjaja, J. Y. P. Ko, Z. Bacsik, B. Aziz, L. J. Liu, Y. F. Hu, L. Bergstrom, C. W. Tai, T. K. Sham, M. Eden, N. Hedin, *Angew. Chem. Int. Ed.* **2010**, *49*, 8889–8891.
[17] a) M. W. Berchtold, H. Brinkmeier, M. Muntener, *Physiol. Rev.* **2000**, *80*, 1215–1265; b) Y. Yaoita, *Front. Endocrinol.* **2019**, *10*, 143; c) A. Martinez, C. K. Lam, V. von Tscharner, B. M. Nigg, *Physiol. Rep.* **2019**, *7*, e13990; d) U. Pohl, *Physiol. Rev.* **2020**, *100*, 525–572.
[18] a) O. Hardt, K. Nader, L. Nadel, *Trends Cogn. Sci.* **2013**, *17*, 111–120; b) C. T. Yu, H. L. Guo, K. P. Cui, X. Y. Li, Y. N. Ye, T. Kurokawa, J. P. Gong, *Proc. Natl. Acad. Sci. USA* **2020**, *117*, 18962–18968.
[19] R. L. Davis, Y. Zhong, *Neuron* **2017**, *95*, 490–503.
[20] E. Palleau, D. Morales, M. D. Dickey, O. D. Velev, *Nat. Commun.* **2013**, *4*, 2257.

Manuscript received: July 17, 2023
Accepted manuscript online: September 6, 2023
Version of record online: ■■, ■■

Research Articles

Hydrogels

H. Wang, X. Fu, G. Gu, S. Bai, R. Li, W. Zhong, X. Guo, R. Eelkema, J. H. van Esch, Z. Cao,* Y. Wang* _____ e202310162

Dynamic Growth of Macroscopically Structured Supramolecular Hydrogels through Orchestrated Reaction-Diffusion

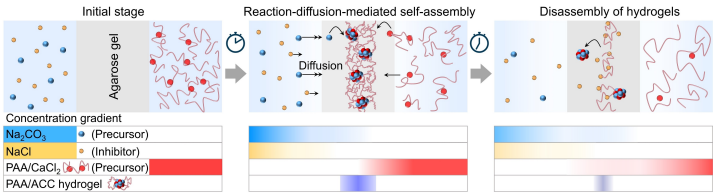

Dynamic growth of structured supramolecular hydrogels has been achieved by a simple reaction-diffusion strategy, reminiscent of the dynamic structural evolution of living organisms. The dynamic growth of the hydrogel has been well explained by a reaction-diffusion model, which provides a robust approach to program the growth of diverse dynamic hydrogel structures.